Non-coding RNA Research 10 (2025) 130–139

Contents lists available at ScienceDirect

Non-coding RNA Research

journal homepage: www.keaipublishing.com/en/journals/non-coding-rna-research

Original Research Article

# MiR-204-5p overexpression abrogates Dacarbazine-induced senescence in melanoma cells in vivo MiR-204-5p abrogates senescence

Ekaterina Lapkina [a], Ivan Zinchenko [a], Viktoriya Kutcenko [a], Eugeniya Bondar [b,c,d], Andrey Kirichenko [e], Irina Yamskikh [b,c,d], Nadezhda Palkina [a], Tatiana Ruksha [a,*]

[a] Department of Pathophysiology, Krasnoyarsk State Medical University, Krasnoyarsk, Russia
[b] Department of Genomics and Bioinformatics, Institute of Fundamental Biology and Biotechnology, Siberian Federal University, Krasnoyarsk, Russia
[c] Laboratory of Forest Genomics, Institute of Fundamental Biology and Biotechnology, Siberian Federal University, Krasnoyarsk, Russia
[d] Laboratory of Genomic Research and Biotechnology, Federal Research Center "Krasnoyarsk Science Center" Siberian Branch, Russian Academy of Science, Krasnoyarsk, Russia
[e] Department of Pathological Anatomy, Krasnoyarsk State Medical University, Krasnoyarsk, Russia

ARTICLE INFO

*Keywords:*
Dacarbazine
DTIC
Drug resistance
Melanoma
miR-204-5p
NGS
Senescence
Transcriptome

ABSTRACT

Cancer cell drug resistance hinders significantly therapeutic modalities in oncology. Dacarbazine is chemotherapeutic agent traditionally used for melanoma treatment although it's effectiveness insufficient. In the present study we performed NGS-based transcriptomic profiling of B16 melanoma tumors after Dacarbazine treatment in vivo. Whole transcriptome sequencing revealed 34 differentially expressed genes most of them associated with drug resistance and apoptosis evading. In accordance to bionformatic analysis, 6 signaling cascades: "D-Amino acid metabolism", "NF-kappa B signaling pathway", "Phosphatidylinositol signaling system", "P53 signaling pathway", "IL-17 signaling pathway" and "Bile secretion" were enriched by differentially expressed genes. Next we provided a combined treatment by Dacarbazine and miR-204-5p mimic as miR-204-5p was considered previously implicated in cancer drug resistance. This approach lead to an increase of miR-204-5p expression in B16 melanoma cells in vivo that was accompanied by subsequent decrease in the expression of miR-204-5p target genes – *BCL2* and *SIRT1* in the primary tumors. MiR-204-5p overexpression with Dacarbazine application resulted in increased the weight, and volume of primary tumors and diminished the proportion of β-Galactosidase expression in melanoma B16-bearing mice. Taking together, our study revealed that although miR-204-5p showed antiproliferative capacities in vitro, it's mimic in combination with Dacarbazine is able to potentiate tumor growth triggering probably a switch from senescent to proliferative phenotype of malignant cells.

## 1. Introduction

Metastatic melanoma is the most aggressive malignant neoplasm of the skin. Chemotherapy, targeted therapy, surgical excision, and immunotherapy are used to treat metastatic melanoma. Although chemotherapy remains an established treatment for metastatic melanoma, drug resistance often develops to anticancer drugs, leading to treatment failure. Therefore, the search for ways to overcome drug resistance continues to be an urgent task [1].

One of the drugs considered as a standard chemotherapy for melanoma is an alkylating agent Dacarbazine (DTIC). DTIC is well known monotherapy agent for the treatment of advanced metastatic melanoma and has been part of the melanoma standard chemotherapy regimen for more than 30 years. Unfortunately, response rates to DTIC monotherapy are dismally low, ranging from 10 % to 20 %, with complete responses observed in less than 5 % of patients with disseminated forms of a tumor [2]. DTIC was originally developed as an antimetabolite drug being analogue of 5-aminoimidazole-4-carboxamide, an intermediate in purine biosynthesis. However, its cytotoxic activity is due to the formation of methyldiazonium during its conversion, which methylates DNA [3].

DTIC induces the generation of cytotoxic O6-chloroethylguanine DNA by formation of adducts with subsequent cross-links between the

* Corresponding author.
*E-mail addresses:* e.z.lapkina@mail.ru (E. Lapkina), Zinchenko.Ivan.003@gmail.com (I. Zinchenko), vika.kucenko@mail.ru (V. Kutcenko), bone-post@yandex.ru (E. Bondar), krasak.07@mail.ru (A. Kirichenko), iyamskikh@mail.ru (I. Yamskikh), Mosmannv@yandex.ru (N. Palkina), tatyana_ruksha@mail.ru (T. Ruksha).

https://doi.org/10.1016/j.ncrna.2024.09.009
Received 20 April 2024; Received in revised form 16 September 2024; Accepted 16 September 2024
Available online 21 September 2024

chains followed by an inhibition of DNA replication or RNA transcription, which leads to cell cycle arrest in the G2 phase. The enzyme O6-alkylguanine-DNA-alkyltransferase (MGMT) helps in the restoration of these adducts, thus impairing the cytotoxic effect and acting as a powerful factor in tumor cell resistance [4]. DTIC was found to induce a weak apoptotic response, both alone and in combination with other chemotherapeutic agents cisplatin and vinblastine [5].

Numerous mechanisms were described as favoring tumor drug resistance including epigenetic modifications that are govern by microRNAs [6]. Being regulators at the post-transcriptional level, microRNAs are small non-coding RNAs that usually repress gene expression by causing mRNA degradation or suppressing mRNA translation through sequence-specific interactions with 3′-untranslated regions of mRNA [7]. Each type of microRNA can have up to hundreds of different types of target mRNAs and, conversely, several genes can be regulated by one type of microRNA [8]. The first data regarding the role of microRNAs in carcinogenesis was obtained by the scientific group of C. Croce using a model of chronic lymphocytic leukemia. Since then, the number of studies regarding the involvement of microRNAs in various processes associated with carcinogenesis has expanded significantly [9–11]. The regulatory role of these molecules in relation to the cell cycle dynamics, apoptosis, DNA repair, the functioning of tumor suppressors, tumor cell migration, invasion, immune evasion, and chemoresistance has been demonstrated [12,13].

The ability of microRNAs to modulate cancer cell survival under specific treatment can be a favorable factor for overcoming melanoma drug resistance. MiR-204-5p involvement in a drug resistance regulation has been shown in various malignant tumors – hepatocellular carcinoma [14], neuroblastoma [15], colorectal cancer [16], squamous cell carcinoma [17]. It recently was shown that miR-204 by inhibiting CD44 signal pathway suppresses non-small lung cancer cells epithelial mesenchymal transition and reduces stem cell phenotype potentiating sensitivity to epidermal growth factor receptor inhibitor osimertinib [18]. In chronic myelogenous leukemia cells miR-204-5p inhibited *MYC* downstream gene which induced β-catenin translocation into the nucleus activating multidrug resistance gene 1 (*ABCB1*) resulting in imatinib resistance [19].

As stated earlier, according to our preliminary results [20] and a number of other studies [21,21], miR-204-5p and its homologue miR-211 are among the most differentially expressed miRNAs in melanoma and benign melanocytic neoplasms. Additionally, a publication by C. Croce and S. Volinia identified downregulation of miR-204-5p in melanoma cells as «a key event in melanoma pathogenesis » [22]. Fattore L. et al. showed that miR-204-5p overexpression in a combination with oxyplatine exerts antitumor effects in BRAF inhibitor vemurafenib-resistant melanoma cells by targeting chemokine ligand 5 via activating downstream AKT signaling and blocking serin-threonine proteinkinase GSK-3 [23].

Although numerous data showed that the expression levels of some microRNAs are associated with the effectiveness of chemotherapy, opposite, the mechanisms associated with the development of melanoma chemoresistance have not yet been revealed, and the role of microRNAs in these processes has not been fully identified [24,25].

Therefore, the goal of this study was to determine if microRNA miR-204-5p overexpression in melanoma cells in vivo potentiate the effectiveness of melanoma therapy by DTIC.

## 2. Materials and methods

### 2.1. Animals

Female C57Bl6 mice aged 6–8 weeks were purchased from the Federal State Budgetary Institution “Rappolovo Laboratory Animal Nursery” of the National Research Center “Kurchatov Institute” (St. Petersburg, Russia).

The animals were kept in a specialized vivarium at room temperature under natural light conditions with free access to water and food. Mice were randomly divided into 4 groups for experimental treatment: Control (n = 12), DTIC (n = 12), DTIC + Negative Control (n = 12), DTIC + miR-204-5p Mimic (n = 12), (Fig. 1).

### 2.2. In vivo modeling of melanoma

The study was approved by the Local Ethics Committee of the Krasnoyarsk State Medical University (approval no 116/2022, date issued: 27.12.2022). The study was carried out according to the recommendations in the National Institute of Health’s Guide for the Care and Use of Laboratory Animals (website ncbi.nlm.nih.gov/books/NBK54050).

Before the experiment, the mice were adapted to the conditions of the vivarium, the period of adaptation was at least 2 weeks. The average weight of mice at the beginning of the experiment was 16.0 g.

B16 melanoma cells were kindly provided by the Research Institute of Fundamental and Clinical Immunology (Novosibirsk, Russia). For subcutaneous implantation, thawed melanoma cells B16 in a concentration of $1{,}5 \times 10^6$ in a volume of 0.5 ml Hanks Solution (HBSS) (Gibco, ThermoFisher Scientific, USA) were injected subcutaneously in the form of a papule into the right side of the abdomen.

### 2.3. DTIC treatment of melanoma B16-bearing mice

On day 7 after tumor transplantation, mice with subcutaneous palpable tumors were randomly divided into 4 groups for experimental treatment with DTIC. Group 1 «Control», n = 12, animals in this group were intraperitoneally injected with phosphate buffered saline (PBS) in a volume of 250 μl. Group 2 «DTIC», n = 12, animals in this group were intraperitoneally injected with a solution of DTIC (DTIC) (Sigma-Aldrich, USA) in PBS at a concentration of 50 mg/kg of animal weight. The dosage regimen and frequency of administration of DTIC were selected according to the average values most often used [26,27]. Injections with DTIC and PBS were carried out three times on days 8, 10 and 12 after melanoma cell transplantation. On day 14, mice were sacrificed for further analysis of primary tumors and organs.

### 2.4. Combination of DTIC and c mir-204-5p mimic application in melanoma B16-bearing mice

For combined treatment with DTIC and mimic, two more groups of mice were randomly formed on the 7th day after tumor transplantation into mice with subcutaneous palpable tumors. Group 3 «DTIC + Negative Control», n = 12, and group 4 «DTIC + miR-204-5p mimic», n = 12, animals in these groups were intraperitoneally injected with a solution of DTIC in phosphate buffer at a concentration of 50 mg/kg in combination with the administration of 5 nMol of mimic Negative Control (designed as a random set of nucleotides and in this experiment is represented by the sequence: CGUACUCUCUCUUCACUUCUUG) (DNA-Sintez, Moscow, Russia) in group 3 and 5 nmol miR-204-5p mimic (RNA sequence: UUCCCUUUGUCAUCCUAUGCCU) (DNA-Sintez, Moscow, Russia) in group 4. Invivofectamine® 3.0 Reagent (Invitrogen, ThermoFisher Scientific, USA) was used to perform transient transfection. Injections in all study groups were carried out three times – on days 8, 10 and 12 after transplantation of melanoma B16 into mice. The experiment was finalized on a day 14th after melanoma transplantation. Then animals of all groups were euthanized. Primary tumors and distant organs that are targets of melanoma metastasis – lungs and livers, were processed for further investigation.

### 2.5. Tumor growth dynamics in vivo

The weight of the animals, as well as the size of the tumors in B16 melanoma-bearing mice were measured daily. Tumor volume ($mm^3$) was determined as follows: Tumor volume ($mm^3$) = (tumor length x

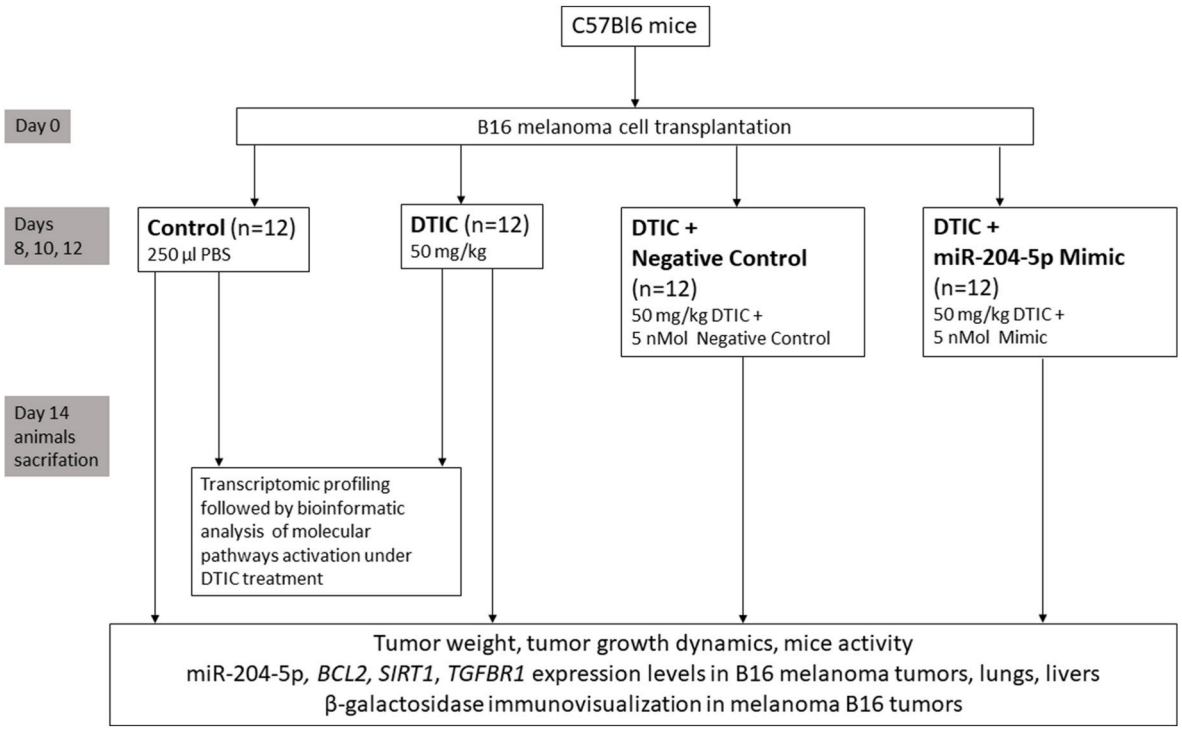


**Fig. 1.** Experimental design.

tumor width$^2$) x 0.5. The growth inhibition index (%) was defined as: (mean volume of treated tumor – mean volume of Control tumor)/mean volume of Control tumor x 100. To assess the effect of the treatment on the activity of mice in terms of the toxic effect of administered substances, the activity index of animals in observation groups was assessed by daily assigning points to each mouse on the following scale: 0 – the mouse died, 1 – coma with lack of response to tactile stimuli, 2 – minimal motor activity with active movements, including weak, mostly involuntary reactions to tactile stimuli, 3 – slow movement (the animal takes several steps only when pushed) with an "avoidance" reaction to tactile stimuli, 4 – subnormal motor activity in the form of slow active movements around the cage, reaction to tactile stimuli is "avoidant-defensive with attempts to bite", 5 – normal motor activity, active movement around the cage, reaction to tactile stimuli – "avoidance with pronounced defensive reactions".

Primary melanoma tumors were isolated, as well as distant organs – distant targets of melanoma metastasis – lungs and livers. The organs were carefully examined using a magnifying glass to identify metastases. The volumes and weights of isolated tumors were measured. Next, part of each tumor and organ was fixed in an RNA-stabilizing solution IntactRNA (Evrogen, Moscow, Russia) for molecular genetic methods, and the other part in a 10 % neutral buffered formalin solution for further immunohistochemical methods.

### 2.6. Real time PCR

Isolation of total RNA from cells and tissues was carried out using a DiaGen reagent kit. (Dia-m, Moscow, Russia). The reverse transcription (RT) reaction was performed using the MMLV RT kit (Evrogen, Russia) according to manufacture's instructions. For this purpose, 1.5 µl of a specific 5xRT primer from the corresponding microRNA expression kits (cat. no. 4427975, Applied Biosystems, USA) or 1.5 µl of a random decanucleotide primer from the MMLV RT kit to determine mRNA levels, was added to each sample consisting of 3 µl of total RNA. The reverse transcription reaction for each sample was performed for 50 min at 37 °C in a 5.5 µl reaction mixture consisting of 1 µl dNTP mixture, 1 µl DTT (1,4-dithiothreitol), 2 µl 5xfirst standard buffer, 0.5 µl of MMLV reverse transcriptase and 1 µl of nuclease-free water, at 37 °C for 50 min.

cDNA amplification was performed on a StepOne™ Real-Time PCR-System (Applied Biosystems, Singapore) using 2 µl per sample with the following thermocycling conditions: 50 °C for 2 min, 95 °C for 10 min; and 40 cycles of 95 °C for 15 s and 60 °C for 1 min. The fluorescent signal of carboxy-X-rhodamine (ROX) was subsequently detected. The reaction mixture used to determine the expression of both microRNA and mRNA in a total volume of 18 µl consisted of 1 µl 20× specific primers, 8 µl 2.5-fold reaction mixture for RT-qPCR in the presence of ROX (Syntol, Moscow, Russia) and 9 µl nuclease-free water. Used reagent kits containing 20× specific primers to determine mRNA expression in mice: Masp1 (Ensembl: ENSMUSG00000022887), Ccng1 (Ensembl: ENSMUSG00000020326), Mmp12 (Ensembl: ENSMUSG00000049723) (DNK-sintez, Russia), Tyr (Mm00495817_m1), SIRT1 (Mm00490758_m1), BCL2 (Mm00477631_m1) and TGFBR1 (Mm00436964_m1) (Applied Biosystems, USA), 20× specific primers ACTB – actin beta (Mm02619580_g1) and HPRT1 – hypoxanthine phosphoribosyltransferase 1 (Mm02800695_m1) (Applied Biosystems, USA) were used as endogenous Controls. To assess the expression of microRNA miR-204-5p, 20× primers (00508, Applied Biosystems, USA) were used, and primers for short non-coding RNA U6 (001973) and snoRNA234 (AF357329 001234) (Applied Biosystems, USA) were used as endogenous Controls.

The relative expression of miRNA was calculated by using the $2^{-\Delta\Delta Ct}$ method for cell samples and the $2^{-\Delta Ct}$ method for tissue samples and was expressed as a fold-change [28]. To determine the expression level simultaneously for several endogenous normalizing Controls, the geometric mean of the product of expression levels was calculated.

### 2.7. Immunostaining

Immunohistochemistry was performed using the Mouse and Rabbit Specific HRP/AEC IHC Detection Kit – Micropolymer (ab236467, Abcam, USA). For this purpose, the sections were deparaffinized in xylene and dehydrated in ethanol gradients, then washed twice in PBS. Unmasking was proceeded in citrate buffer (pH 6.0) at t +103 °C for 30 min. Primary antibodies to Ki-67 (cat. no. MA5-14520, Invitrogen, USA)

were used at a dilution of 1:100, and primary β-Galactosidase antibody (anti-GLB1) (cat. no. ab203749, Abcam, USA) were used at a dilution of 1:250. Slides were incubated for 1 h at room temperature. Immunostaining was visualized using the dye 3-Amino-9-ethylcarbazole (AEC Single Solution). Negative Controls were proceeded similarly but without the primary antibody. Positively stained cells were evaluated using an Olympus BX-41 microscope (Olympus Corporation, Tokyo, Japan) and Infinity 2 Lumenera camera (Lumenera Corporation, Ottawa, Canada). Images were analyzed using Infinity Capture and Infinity Analyze software (version 6.5.2, Lumenera Corporation, Ottawa, Canada). The slides were viewed at a magnification of × 400, and 10 fields were randomly selected for further analysis of antigen expression. The number of $GLB1^+$ cells was determined per 100 cancer cells.

### 2.8. Transcriptomic profiling by next generation sequencing

Total RNA of melanoma tumors obtained from mice of a Control and DTIC groups were extracted using TRIzol® reagent (Qiagen, Hilden, Germany) and RNeasy Mini Kit (Quiagen, Hilden, Germany). The RNase inhibitor RiboLock (Thermofisher, USA) was added to the isolated RNA. The quality of the isolated total RNA was checked on a Qsep400 instrument (BiOptic, BiOptic, New Taipei City, Taiwan, Taiwan) using the RNA Cartridge Kit R1-O-4CH (BiOptic, BiOptic, New Taipei City, Taiwan, Taiwan). The amount of isolated RNA was measured using a Qubit RNA High Broad Range kit (Thermo Fisher Scientific, Eugene, USA).

RNA library preparation and NGS were performed by Evrogen (Russia). For transcriptome sequencing, library construction was carried out in several stages. First, to enrich the mRNA fraction according to the poly-A principle, particles with poly-T tails (Shenzhen, China) were used, to which 200 ng of total RNA was added. Next, the mRNA molecules were fragmented to small sizes. Reverse transcription was performed on these fragments using random primers (Shenzhen, China). The second strand cDNA was synthesized with dUTP instead of dTTP. The resulting double-stranded cDNA was subjected to end repair and 3′-end polyadenylation (Shenzhen, China). Adapter ligation was then performed (Shenzhen, China). The next step was cleavage of the uracil-labeled second strand using the enzyme uracil DNA glycosylase (UDG) (Shenzhen, China), followed by PCR amplification (SimpliAmp™ Thermal Cycler, Thermo Fisher Scientific, Eugene, USA).

Library quality Control was carried out using a Qsep400 instrument (BiOptic, New Taipei City, Taiwan). Then, the libraries were cyclized, amplified to create nanoballs, and sequenced on the DNBSeq platform using DNBSeq technology on a DNBSeq G-400 instrument (Shenzhen, China) in 100-bp paired-end sequencing mode generating at least 40 million data per sample. Data with adapter sequences or low quality sequences were filtered using SOAPnuke software developed by BGI [29].

### 2.9. Bioinformatic analysis

Quality of reads was assessed with FastQC (website bioinformatics.babraham.ac.uk/projects/fastqc/). Reads were mapped to the GRCm39 assembly of Mus musculus reference genome using HISAT2, the mapped reads were quantified using htseq-count. Differentially expressed genes were identified based on the negative binomial distribution using DESeq2. Contrasts were set to « DTIC » vs « Control» and the threshold of absolute value of log2 fold-change ≥0.5 was implemented into hypothesis testing with the results function from DESeq2.

Contrasts were established (DTIC), and an absolute value threshold of log2 fold change ≥0.5 was implemented in hypothesis testing using the outcome function from DESeq2.

The Benjamini–Hochberg false discovery rate was utilised to Control Type I error rate in multiple testing, and genes with adjusted P-value <0.05 and absolute value of log2 fold-change ≥0.5 were considered to be differentially expressed (DEGs). These DEGs were further used to perform gene ontology (GO) enrichment analysis using ShinyGO (website doi.org/10.1093/bioinformatics/btz931) and infer protein-protein interactions.

To predict miR-204-5p and miR-211 target genes by bioinformatic analysis, three computational tools were used – miRDB (website//mirdb.org/), DIANA-TarBase v7 (website//diana.imis.athena-innovation.gr/DianaTools/index.php?r = tarbase/index) and the DIANA-microT-CDS v.5 database (website//dianalab.e−ce.uth.gr/html/dianauniverse/index.php?r = microT_CDS), which is trained on positive and negative microRNA recognition sets (MREs) located in both the 3′-UTR and CDS.

### 2.10. Statistical analysis

Statistical analysis was performed using software package Statistica 7.0 (StatSoft, Russia). To assess the normality of distribution, the Kolmogorov-Smirnov test was used. Since all the samples we analyzed did not have a normal distribution, the non-parametric Mann-Whitney *U* test was used when making a pairwise comparison of data from the study groups. Comparison of the genome sequencing results of the studied samples was carried out using the ANOVA test, corrected using the Benjamini-Hochberg false discovery rate (FDR). The differences were considered as significant if the $p < 0.05$ level. Data are presented as mean and standard errors of the mean (M ± m).

## 3. Results

### 3.1. DTIC treatment did not alter tumor growth in melanoma B16 bearing mice

The activity of B16-melanoma bearing mice upon a treatment with DTIC was stable up to the day 11th and then activity showed a tendency to be decreased slightly in animals treated by DTIC and a combination of DTIC and NC although did not achieve statistical significance. The appearance of animals treated with DTIC also did not differ significantly from animals from the Control group (Fig. 2A and B).

The weight of animals gradually increased during the experiment both in the Control group and in the DTIC treatment group, no differences were found between the groups; the weight gain of mice by the end of the experiment in the DTIC-treated animals was 0.11 g, and in the control group – 0.3 g (Fig. 2C).

Tumor volumes in the Control group and the DTIC-treated animals group increased steadily during the treatment but without significant differences between the groups. The mean tumor weight in the Control group was 0.50 ± 0.15 g whereas in experimental group the weight was 0.31 ± 0.13 g. The mean tumor volume of control group animals was 274.61 ± 56.6 $mm^3$ whereas the mean tumor volume in the DTIC-treated animals group was 322.66 ± 168.06 $mm^3$ (Fig. 2E and F). No difference in tumor weights and volumes between control and experimental groups were found that corresponds to a resistance upon DTIC treatment.

### 3.2. Whole transcriptome sequencing revealed 33 genes with altered expression under DTIC treatment

Transcriptome analysis of primary melanoma B16 tumors under DTIC treatment and Contros was performed by next generation sequencing technology. According to bioinformatics analysis, 33 differentially expressed genes were identified in tumors of DTIC-treated animals versus controls (Table 1).

Among them, 10 genes were downregulated, and 23 were upregulated (Fig. 3A and B). To validate the sequencing results, *MASP1, CCNG1* и *MMP12* expression was assessed using RT-PCR. The RT-PCR data on gene expression corresponded to sequencing results. *MASP1* and *MMP12* levels were increased 2.71-fold and 2.72-fold in accordance to NGS in DTIC-treated tumors versus Controls. RT-PCR analysis revealed *MASP1*

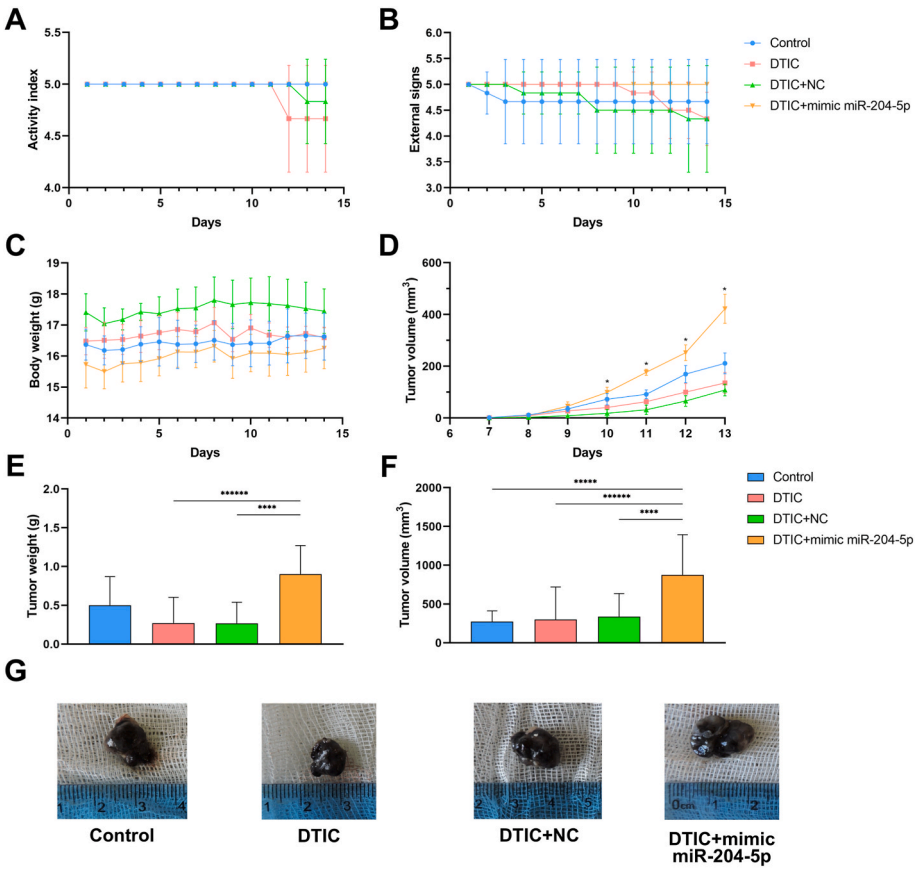


**Fig. 2. Results of treatment with DTIC and miR-204-5p mimic in B16 melanoma-bearing mice.** (A) Mice activity dynamics assessed in accordance with the point activity scale where maximum score is 5 points. (B) Mice appearance score under treatment of DTIC and a combination of DTIC and miR-204-5p mimic. (C) Dynamics of mice body weight under DTIC treatment and a combination of DTIC and miR-204-5p mimic. (D) Dynamics of melanoma tumor volumes in mice under DTIC treatment and a combination of DTIC and miR-204-5p mimic. (E) Mean values of tumor weight and volumes in melanoma B16-bearing mice under treatment with DTIC, DTIC and miR-204-5p mimic (f) Photograph showing melanoma B16 tumors in mice of the study groups. *P < 0.05 in «DTIC » vs « Control»; **P < 0.05 in «DTIC + NC» vs « DTIC»; ***P < 0.05 in «DTIC + NC», vs « DTIC »; ****P < 0.05 in «DTIC + mimic», vs « DTIC + NC»; *****P < 0.05 in «DTIC + mimic » vs « Control»; *****P < 0.05 in «DTIC + mimic » vs « DTIC».

and *MMP12* 3.6 and 9.2 times down-regulation subsequently (p = 0,0495). *CCNG1* expression was increased 1.52 times in accordance to NGS, RT-PCR revealed 5,5 times increase in B16 melanoma of DTIC-treated animals versus Controls (p = 0,0495) (Fig. 3C).

### 3.3. Molecular pathways activation by DTIC treatment are associated with DNA damage, apoptosis regulation, and drug resistance

Differentially expressed genes in melanoma B16 tumors under DTIC treatment belonged to a processes of a cell response to DNA damage (increased expression of the *CCNG1*, *PLCD4* and *PIERCE1* genes was noted), regulation and initiation of the apoptotic process, including regulators of internal signaling pathway of p53-dependent apoptosis and proliferation (the expression of the genes *PIDD1*, *DDIAS*, *ESA2R*, *DDIT4L* increases and *GNG2* decreases), and drug resistance (*ABCC2)*.

Genes with altered expression under DTIC treatment has been identified, which were associated with a regulation of the cytoskeleton organization (up-regulated *MAP3K20*, down-regulated *TNNT2* and S100A8), alpha-tubulin binding (up-regulated *HSPHL*), focal adhesion processes (up-regulated *SERPINB8*, down-regulated *KIRREL3* and S100A9), membrane proteins (down-regulated *KIRREL3*, up-regulated *KLHDC7A*), intercellular communication and exocytosis (up-regulated *DGKI*).

In accordance to bionformatic analysis, differentially expressed genes obtained from DTIC-treated B16-melanoma bearing mice were associated with hyperactivation of the following signal transduction mechanisms: “D-Amino acid metabolism”, “NF-kappa B signaling pathway”, “Phosphatidylinositol signaling system”, “P53 signaling pathway”, “IL-17 signaling pathway” and “Bile secretion”.

Melanoma is highly plastic and heterogeneous tumor where micro-RNA miR-204-5p has been shown as implicated in chemoresistance [28, 29]. Therefore, then we applied synthetic analogue (mimic) of miR-204-5p to decrease chemoresistant melanoma cells subpopulations during DTIC therapy.

### 3.4. MicroRNA-204-5-p mimic application resulted in mir-204-5p overexpression in melanoma tumors of B16-bearing mice

MiR-204-5p expression in B16 melanomas upon DTIC administration increases 7.47 times (p = 0.022) as compared to the Control. MiR-204-5p expression increased 33.8-fold (p = 0.012) in the primary tumors obtained from animals treated with DTIC and miR-204-5p mimic versus tumors of animals treated with DTIC in combination with Negative Control. It indicates the successful delivery of a mimic to the tumor and it’s effective distribution within melanoma cells (Fig. 4A).

The tendency to increase miR-204-5p expression level in lungs of animals treated with a combination of DTIC and mimic was observed as compared to miR-204-5p expression level in lungs of animals treated with DTIC in combination with Negative Control whereas 6.4-fold elevation of miR-204-5p expression level (p = 0.047) was observed as compared to Control group animals. The expression of microRNA miR-204-5p decreased 5.0 times in the livers of animals treated by DTIC

**Table 1**
Differentially expressed genes in melanoma B16 tumors under DTIC treatment according to whole-transcriptome profiling by NGS.

| Gene Name | Log2Fold Change[a] | P-value[b] | Gene Function |
|---|---|---|---|
| Map3k20 | ↑ 1,077 | $1,91 \times 10^{-2}$ | It has kinase activity and affects the organization of the cytoskeleton. |
| Tyr | ↑ 1,749 | $4,69 \times 10^{-5}$ | Controls the formation of melanin. |
| Ccng1 | ↑ 1,525 | $5,11 \times 10^{-6}$ | Regulator of cyclin-dependent protein serine/threonine kinase, involved in DNA repair processes. |
| Dglucy | ↑ 2,081 | $4,35 \times 10^{-2}$ | Participates in glutamate metabolism. |
| Masp1 | ↓ 2,713 | $4,19 \times 10^{-4}$ | This gene activates serine-type endopeptidase and is involved in complement activation via the lectin pathway. |
| Abcc2 | ↑ 3,000 | $1,33 \times 10^{-3}$ | This particular protein belongs to the MRP subfamily and is involved in multidrug resistance. |
| Pidd1 | ↑ 1,782 | $4,29 \times 10^{-2}$ | Activator of cysteine-type endopeptidase involved in the apoptotic process and the extrinsic apoptotic signaling pathway through death domain receptors. |
| Plcd4 | ↑ 2,563 | $2,91 \times 10^{-3}$ | Activator of guanyl nucleotide exchange factor and phosphatidylinositol phospholipase C activity. |
| Serpinb8 | ↑ 1,387 | $2,82 \times 10^{-2}$ | Serine-type endopeptidase inhibitor activator, involved in epithelial cell adhesion and negative regulation of endopeptidase activity. |
| Tnnt2 | ↓ 2,301 | $5,20 \times 10^{-4}$ | Encodes a structural protein of the cytoskeleton. |
| Pierce1 | ↑ 2,666 | $6,15 \times 10^{-10}$ | Takes part in DNA repair. |
| Hsph1 | ↑ 1,590 | $3,62 \times 10^{-7}$ | Participates in alpha-tubulin binding processes. |
| Ddias | ↑ 1,386 | $3,03 \times 10^{-2}$ | Activator of the intrinsic apoptotic signaling pathway in response to DNA damage. |
| Kirrel3 | ↓ 1,890 | $4,48 \times 10^{-2}$ | Membrane protein is involved in the binding of cell adhesion molecules and is an integral component of the membrane. |
| Glce | ↓ 1,046 | $3,85 \times 10^{-2}$ | Participates in the biosynthesis of heparan sulfate proteoglycan and the biosynthesis of heparin. |
| Eda2r | ↑ 2,606 | $3,82 \times 10^{-10}$ | Activator of signaling molecules of the internal signaling pathway of p53-dependent apoptosis. |
| Dnai4 | ↑ 1,470 | $1,50 \times 10^{-3}$ | Takes part in the assembly of dynein motor proteins. |
| Dgki | ↑ 1,627 | $4,48 \times 10^{-2}$ | Participates in the regulation of exocytosis of synaptic vesicles. |
| Rlbp1 | ↑ 1,625 | $3,85 \times 10^{-2}$ | Functional component of the visual cycle. |
| Gng2 | ↓ 0,994 | $2,82 \times 10^{-2}$ | Participates in the binding of the beta subunit of the G protein and GTPase activity, regulates cell proliferation. |
| Ddit4l | ↑ 2,157 | $9,17 \times 10^{-6}$ | Inhibits cell growth by regulating the TOR signaling pathway upstream of the TSC1-TSC2 complex and downstream of AKT1. |
| Inka2 | ↑ 2,422 | $4,06 \times 10^{-4}$ | Provides protein kinase binding activity and protein serine/threonine kinase inhibitor activity. |
| Mmp12 | ↓ 2,721 | $6,62 \times 10^{-7}$ | Encodes a member of the matrix metalloproteinase family. |
| Or4f62 | ↑ 3,098 | $5,11 \times 10^{-6}$ | Olfactory receptor protein. |
| Or4f47 | ↑ 5,297 | $2,82 \times 10^{-2}$ | Olfactory receptor protein. |
| S100a8 | ↓ 4,571 | $3,17 \times 10^{-2}$ | A protein of the calprotectin family, it is involved in the transport of arachidonic acid by leukocytes, modulation of the tubulin-dependent cytoskeleton during phagocyte migration and activation of neutrophil NADPH oxidase. |
| S100a9 | ↓ 4,140 | $3,75 \times 10^{-2}$ | A protein of the calprotectin family, induces chemotaxis and adhesion of neutrophils. |
| Stfa2l1 | ↓ 5,540 | $4,74 \times 10^{-3}$ | Regulates cysteine-type endopeptidase inhibitor activity and protease binding activity. |
| Slc4a5 | ↑ 2,218 | $4,32 \times 10^{-2}$ | Mediates sodium- and bicarbonate-dependent electrogenic cotransport of these molecules. |
| C1qtnf9 | ↓ 2,142 | $2,09 \times 10^{-2}$ | Probable adipokine. Activates the AMPK, AKT and p44/42 MAPK signaling pathways. |
| Mob3b | ↑ 1,363 | $3,82 \times 10^{-10}$ | Regulator of protein kinase activator activity, is involved in the positive regulation of protein phosphorylation. |
| Klhdc7a | ↑ 2,735 | $7,40 \times 10^{-3}$ | Membrane protein. |
| Gm15261 | ↑ 2,177 | $1,49 \times 10^{-2}$ | lncRNA. |

[a] Increased (↑), decreased (↓) in samples from the DTIC treatment group compared to the phosphate buffer treatment group.
[b] P-value level corrected using the Benjamini-Hochberg false discovery rate (FDR).

with mimic as compared to Control group ($p = 0.047$) although no differences in miR-204-5p expression were revealed as compared to Negative Control group (Fig. 4A).

### 3.5. *miR-204-5p mimic induces mir-204-5p target genes BCL2 and SIRT1 down-regulation in melanoma in vivo*

Bioinformatics analysis performed with the use of computational tools miRDB, DIANA-TarBase and DIANA-microT-CDS identified *SIRT1* and *BCL2* ($p < 0,001$) as target genes of miR-204-5p.

MiR-211 is considered to be a homologue of miR-204-5p. Therefore, to evaluate the selectivity of miR-204-5p mimic's effects, we also assessed the expression of the *TGFBR1* gene, which is a target gene of miR-211, but not miR-204-5p. No difference in *TGFBR1* expression was determined between all groups of animals studied.

*BCL2* expression levels increased 5.8-fold ($p = 0.049$) in melanomas of DTIC-treated animals as compared to Control group animals. Combination of DTIC and miR-204-5p mimic did not result in *BCL2* expression levels alterations as compared to *BCL2* expression in tumors of mice treated with a combination of DTIC and Negative Control.

*SIRT1* expression in melanomas was not altered in DTIC-treated animals as compared the Control group animals, while *SIRT1* expression elevation was found in tumors of animals treated by the combination of DTIC and Negative Control versus both Control group and DTIC-treated group ($p = 0.049$). MiR-204-5p overexpression was associated with 4.1-fold decreased expression of *SIRT1* ($p = 0.049$) in animals treated with a combination of DTIC and miR-204-5p mimic as compared to *SIRT1* levels in tumors of animals treated by DTIC and Negative Control (Fig. 4B).

*TGFBR1* gene was not expressed in the lungs of mice of all groups. 31.6-fold decrease of *BCL2* expression ($p = 0.012$) was found in the lungs of animals treated by DTIC. *SIRT1* expression in the lungs of DTIC-treated mice decreased by 3.9 times as compared to expression of a Control group mice ($p = 0.012$). *SIRT1* expression in mice treated with the combination of DTIC and miR-204-5p mimic was 3.8 times lower ($p = 0.012$) than in animals treated by DTIC and Negative Control, but 2.9 times higher ($p = 0.012$) than in DTIC-treated animals, and did not differ with Control group animals (Fig. 4C).

*TGFBR1* expression was increased in the liver of animals treated with DTIC and miR-204-5p mimic versus expression levels in the liver of animals treated with DTIC and Negative Control, versus DTIC-treated

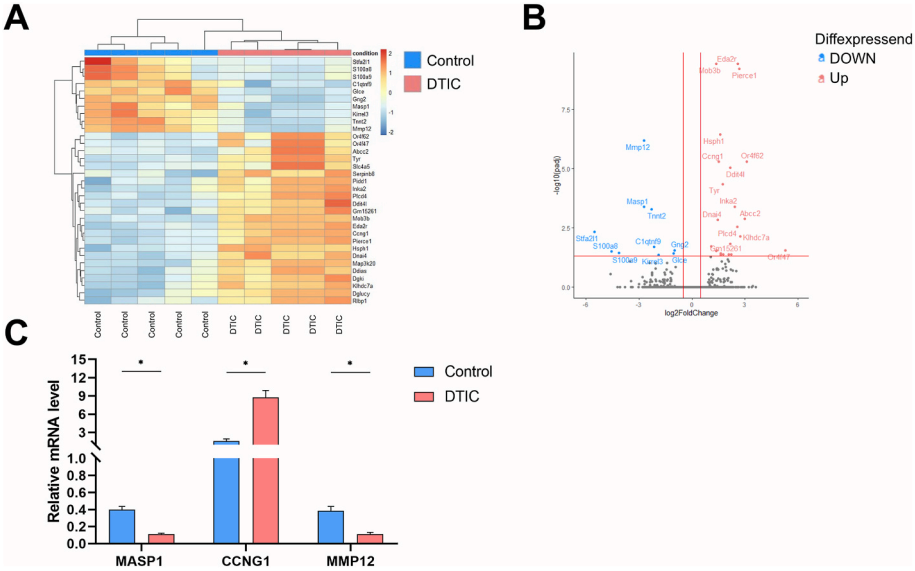


**Fig. 3. Results of full-transcriptomic next-generation sequencing of primary tumors in B16 melanoma-bearing mice (Controls and DTIC-treated animals).** (A) Hierarchical clustering (heat map), demonstrating the grouping of samples between DTIC-treated animals and controls (B) Volcano plot displaying differentially expressed genes. Blue spots represent up-regulated genes in DTIC-treated melanoma cells versus control. Pink spots represent down-regulated genes, FDR≤0,05. (C) Real-time PCR based expression analysis results. *P < 0.05 in «DTIC treated animals group » vs « Control».

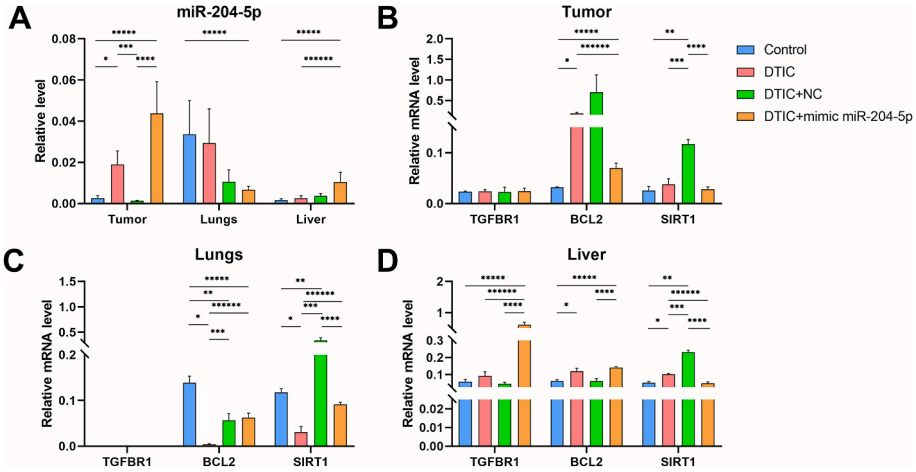


**Fig. 4. MiR-204-5p mimic transfection efficiency into the B16 melanoma cells, as well as into lung and liver cells which are the primary targets of melanoma metastasis.** (A) Expression level of microRNA miR-204-5p in melanoma tumors, lungs and liver according to the results of RT-PCR. (B) Expression levels of target genes *TGFBR1*, *BCL2* and *SIRT1* in the primary melanoma tumor node in the study groups, determined by RT-PCR (C). Expression levels of the target genes *TGFBR1*, *BCL2* and *SIRT1* in the lungs of melanoma B16-bearing mice in the studied groups, determined by RT-PCR. (D) MiR-204-5p target genes *TGFBR1*, B*CL2* and *SIRT1* expression in the livers of melanoma b16 bearing mice, determined by RT-PCR. *P < 0.05 in «DTIC » vs « Control»; **P < 0.05 in «DTIC + NC» vs « DTIC»; ***P < 0.05 in «DTIC + NC», vs « DTIC »; ****P < 0.05 in «DTIC + mimic», vs « DTIC + NC»; *****P < 0.05 in «DTIC + mimic » vs « Control»; *****P < 0.05 in «DTIC + mimic » vs « DTIC».

animals and versus Control group animals (p = 0.012 in all cases).

In liver tissue *TGFBR1* expression did not differ between animals in the Control group and the DTIC treated animals and DTIC with mimic Negative Control treatment group. *BCL2* mRNA expression levels were 2 times higher in the liver of animals treated with DTIC (p = 0.012). *BCL2* expression was 2.3 times higher in the livers of animals treated with DTIC and miR-204-5p mimic as compared to *BCL2* expression levels in livers of animals treated with DTIC in combination with the Negative Control and in the group of animals treated with Control (p = 0.012 in both cases). *SIRT1* expression decreased in the livers of animals treated with combination of DTIC and miR-204-5p mimic as compared to the SIRT1 mRNA levels in the livers of animals treated with DTIC and Negative Control (p = 0.012) (Fig. 4D).

### *3.6. miR-204-5p overexpression in combination with DTIC facilitates a growth of melanoma tumors*

Mice treated with DTIC, combination of DTIC and miR-204-5p mimic or Negative Control throughout the whole experiment had no differences in activity and appearance between groups studied (Fig. 2A and B). However, body weight increase was registered in all groups at the end of experimental treatment. There were no differences in the weight of mice between the groups (Fig. 2C). Maximal body weight increase was determined in the group of animals treated by a combination of DTIC and miR-204-5p mimic where weight gain was 0.53 g, while the weight gain in the group of animals treated by DTIC and Negative Control was 0.04 g, in DTIC-treated animals – 0.11 g, and in a Control group mice – 0.3 g. The highest tumor volume gain in the group of

animals treated by a combination of DTIC and miR-204-5p mimic ($p = 0.025$) (Fig. 2D). Again, tumor weight was the highest in the groups of animals treated with a combination of DTIC and miR-204-5p mimic versus tumor weight rates in animals treated with a combination of DTIC and negative Control as well as treated by DTIC ($p = 0.016$) (Fig. 2E). Tumor volume was 2.6 times higher in the group of animals treated by a combination of DTIC and miR-204-5p mimic versus tumor volumes in the animals treated with DTIC and Negative Control ($p = 0.037$), increased 2.7-fold as compared to tumor volumes of DTIC-treated animals ($p = 0.025$), and 3.2-fold times versus Control ($p = 0.037$) (Fig. 2F and G).

### 3.7. DTIC-induced β-galactosidase overexpression is abolished by mir-204-5p mimic in B16 melanoma cells in vivo

As reported previously, DTIC induces cancer cell senescence. Therefore, we evaluated β-Galactosidase expression in the mice B16 melanoma tumors. We revealed that DTIC induced 5.2 fold increase of β-Galactosidase positive cells as compared to the group of animals treated with a control ($p < 0.001$). Besides, melanoma B16 tumors demonstrated diminished 4.5 times β-Galactosidase levels in a group of animals treated by a combination of DTIC and miR-204-5p mimic as compared to the animals treated by a Negative Control ($p = 0.049$) and 3.9 times decrease ($p = 0.005$) versus animals treated with DTIC (Fig. 5).

## 4. Discussion

MicroRNA molecules have shown to be implicated in the regulation processes associated with the development of drug resistance. Several microRNAs can control drug response in cancer cells through p53 signaling [13]. The experimental use of inhibitors or microRNA mimics revealed to counteract chemoresistance and demonstrated a synergistic effect with other anticancer drugs. Thus, the application of a doxorubicin-conjugated miR-21 inhibitor encapsulated in star-branched copolymers resulted in a ninefold reduction in tumor volume compared with treatment with either miR-21 or doxorubicin alone [30]. A combination of miR-29b mimic and bortezomib, an anticancer drug used for multiple myeloma treatment, showed that miR-29b via SP1 transcription factor can induce cell sensitivity to bortezomib and stimulate apoptosis through the PI3K-AKT signaling pathway [31].

Therefore, in the present study we applied miR-204-5p specific mimic in combination with DTIC. Indeed, we achieved an increase of miR-204-5p levels in the tumors of melanoma B16-bearing mice as well as down-regulated expression of it's putative target gene *SIRT1*. Opposite, we did not observe *TGFBR1* expression alterations identified as a target gene of miR-211 (which is a homologue of miR-204-5p) but not miR-204-5p [32,33] that confirms selectivity of mimic's action. Altogether these results allowed to summarize that miR-204-5p mimic reached melanoma cells in vivo. However, we observed miR-204-5p target genes levels up-regulation in distant organs, in particular *BCL2* in livers of B16 melanoma-bearing mice. We suppose that it can be due to non-canonical effects of microRNAs. It has been reported previously that some microRNAs can be destabilized as a result of their specific interactions with target mRNA, these transcripts contain sequences that have an almost perfect match with microRNA and contain centered mismatches. This type of interaction causes unloading of the microRNA from AGO and destabilization of the 3′ end of the miRNA. This post-transcriptional regulation of microRNAs is referred as target-directed microRNA degradation [34].

In addition, a study of Lin et al. has been reported that *BCL2* is a highly complementary target for miR-204-5p in prostate cancer cells, having a high binding energy upon binding [35]. Therefore, target-directed microRNA degradation of the administered mimic miR-204-5p can result in a low level of miR-204-5p expression that were detected in distant organs.

Altogether, miR-204-5p mimic interacted differently in normal and in cancer cells that call more attention and needs further investigation to archive systemic effect of microRNAs modulators.

In the present study we determined the evident tumor volumes and weight increase in the group of animals treated by a combination of DTIC and miR-204-5p mimic. In terms of non-canonical mechanisms of regulation by microRNAs it is possible to suggest that tumor volume and weight increase can be explained by the ability of the mimic not to reduce but to increase the expression of certain genes by interacting with reverse complementary sequences in their transcription start sites. Such interactions were reported for p21 as overexpression of miR-1236-3p and miR-370-5p that binding to corresponding sites in the p21 promoter was associated with increased p21 expression in human endometrial cancer, pancreatic cancer, and lung carcinoma cell lines [36].

*SIRT1* as a functional target of miR-204-5p was reported in various types of malignant cells, including cutaneous melanoma [28,37–40]. In prostate cancer cells, miR-204 was found to target *SIRT1*, which is a histone deacetylase, resulting in the reduction of p53 deacetylation. Acetylated p53 triggered a doxycycline-induced mitochondrial apoptosis in prostate cancer cells. These data pointed out an ability of miR-204-5p to stimulate SIRT1/p53 pathway-mediated apoptosis [41]. In our study p53 signal pathway was found as one of the most triggered under DTIC in melanoma tumors of B16-bearing mice according to the results of next-generation whole-transcriptome sequencing. However, we did not observe tumor reduction therefore it is not clear if p53 activation resulted in apoptosis of melanoma cells under DTIC. More likely, p53 signaling pathway activation may result in non-apoptotic

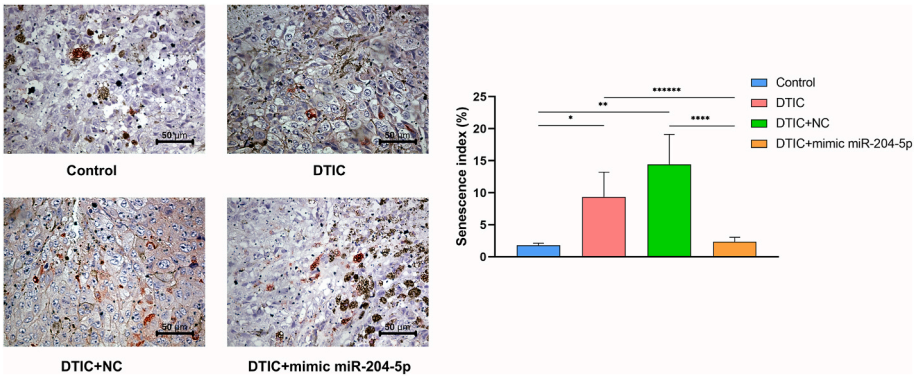


**Fig. 5. Results of assessment of β-Galactosidase expression in primary tumor nodes in mice with transplantable melanoma without specific exposure (introduction of phosphate buffer) and after treatment with DTIC, and with DTIC and miR-204-5p Mimic (magnification × 400).** *P < 0.05 in «DTIC » vs « Control»; **P < 0.05 in «DTIC + NC» vs « DTIC»; ****P < 0.05 in «DTIC + mimic», vs « DTIC + NC»; *****P < 0.05 in «DTIC + mimic » vs « Control»; ******P < 0.05 in «DTIC + mimic » vs « DTIC».

functions of p53 activation [42].

*SIRT1* has been shown to be overexpressed in human melanoma tissues and cell lines, and treatment of melanoma cell lines with Tenovin-1, a *SIRT1* inhibitor, resulted in decreased melanoma cell growth mediated by an overexpression of p53 as well as the cyclin kinase inhibitor p21. Interestingly, p53 was the first nonhistone target discovered for *SIRT1* and was shown later to be an important downstream target of *SIRT1* [43]. In our study we determined a decrease of *SIRT1* expression by miR-204-5p mimic administration to B16 melanoma-bearing mice that did not lead to a decrease in the tumor growth. One explanation could be that numerous target genes interacting with miR-204-5p mimic. In the present study the level of senescent cells producing beta-galactosidase was increased. Notably, treatment of melanoma by a combination of DTIC and miR-204-5p mimic led to a decreasing of β-Galactosidase expression in melanoma cells in comparison to it's levels in melanomas subjected to a treatment by DTIC with Negative Control or DTIC. No difference was found between β-Galactosidase rates in melanomas treated by DTIC and miR-204-5p mimic in comparison to Control. These data correspond to tumor weights that were equal in groups of animals treated by Control and DTIC with miR-204-5p mimic. Thus, it is possible to suggest that miR-204-5p overexpression induces the exit from senescent state. Previously senescence was considered as irreversible cell cycle arrest. Recently there is some data issued confirming that senescent cells can enter to cell cycle again [44]. However, less clear the fate of these cells. We can not suspect their undergoing to apoptosis as tumors did not diminished in their size and volume. Besides, we did not observe specific for apoptotic cells morphology that characterized by cell shrinkage and reduction of a cell size. Senescence features loss under miR-204-5p overexpression in DTIC-treated melanomas may refer to proliferative phenotype switching that forms a basis for cancer cell plasticity.

It can be summarized that miR-204-5p overexpression in combination with DTIC treatment induces the loss of a melanoma B15 senescent phenotype. We expect this treatment application does not have a direct antitumor effect, but has the potential to be used as a tumor cell phenotype switch modulator to overcome drug resistance. Among other things, the non-canonical effects of microRNAs remain underestimated and poorly understood, which increases the level of complexity of the functioning of microRNAs from the point of view of the regulation of carcinogenesis, in particular this concerns miR-204-5p.

## Data availability statement

All relevant data are within the paper and its Supporting Information files. Transcriptomic NGS data have been deposited in the public data repository European Nucleotide Archive (ENA), accession number ERP156937, ArrayExpress (E-MTAB-13737).

## Ethics approval statement

The study was carried out according to the recommendations in the National Institute of Health's Guide for the Care and Use of Laboratory Animals (website ncbi.nlm.nih.gov/books/NBK54050) and was approved by the Local Ethics Committee of the Krasnoyarsk State Medical University (approval no 116/2022, date issued: 27.12.2022).

## Funding statement

The study was supported by a grant from the Russian Science Foundation (project N°.19-15-00110).

## CRediT authorship contribution statement

**Ekaterina Lapkina:** Writing – original draft, Methodology, Investigation, Formal analysis, Data curation. **Ivan Zinchenko:** Visualization, Investigation. **Viktoriya Kutcenko:** Investigation. **Eugeniya Bondar:** Writing – original draft, Software, Methodology, Investigation. **Andrey Kirichenko:** Data curation. **Irina Yamskikh:** Methodology, Data curation. **Nadezhda Palkina:** Writing – review & editing, Writing – original draft, Validation, Supervision, Methodology, Data curation. **Tatiana Ruksha:** Writing – review & editing, Resources, Project administration, Methodology, Funding acquisition, Formal analysis, Data curation, Conceptualization.

## Declaration of competing interest

The authors declare no conflict of interests.

## Appendix A. Supplementary data

Supplementary data to this article can be found online at https://doi.org/10.1016/j.ncrna.2024.09.009.

## References

[1] B. Switzer, I. Puzanov, J.J. Skitzki, L. Hamad, M.S. Ernstoff, Managing metastatic melanoma in 2022: a clinical review, JCO Oncol Pract 18 (5) (2022 May) 335–351, https://doi.org/10.1200/OP.21.00686.

[2] G. Jiang, R.H. Li, C. Sun, Y.Q. Liu, J.N. Zheng, DTIC combined targeted therapy versus DTIC alone in patients with malignant melanoma: a meta-analysis, PLoS One 9 (12) (2014 Dec 11) e111920, https://doi.org/10.1371/journal.pone.0111920.

[3] L. Meer, R.C. Janzer, P. Kleihues, G.F. Kolar, In vivo metabolism and reaction with DNA of the cytostatic agent, 5-(3,3-dimethyl-1-triazeno)imidazole-4-carboxamide (DTIC), Biochem. Pharmacol. 35 (19) (1986 Oct 1) 3243–3247, https://doi.org/10.1016/0006-2952(86)90419-3.

[4] N.J. Hawkins, J.H. Lee, J.J. Wong, C.T. Kwok, R.L. Ward, M.P. Hitchins, MGMT methylation is associated primarily with the germline C>T SNP (rs16906252) in colorectal cancer and normal colonic mucosa, Mod. Pathol. 22 (12) (2009 Dec) 1588–1599, https://doi.org/10.1038/modpathol.2009.130.

[5] R.A. Anvekar, J.J. Asciolla, E. Lopez-Rivera, K.V. Floros, S. Izadmehr, R. Elkholi, et al., Sensitization to the mitochondrial pathway of apoptosis augments melanoma tumor cell responses to conventional chemotherapeutic regimens, Cell Death Dis. 3 (11) (2012 Nov 15) e420, https://doi.org/10.1038/cddis.2012.161.

[6] L. Guo, Y.T. Lee, Y. Zhou, Y. Huang, Targeting epigenetic regulatory machinery to overcome cancer therapy resistance, Semin. Cancer Biol. 83 (2022 Aug) 487–502, https://doi.org/10.1016/j.semcancer.2020.12.022.

[7] A.E. Pasquinelli, MicroRNAs and their targets: recognition, regulation and an emerging reciprocal relationship, Nat. Rev. Genet. 13 (4) (2012 Mar 13) 271–282, https://doi.org/10.1038/nrg3162.

[8] A. Wilczynska, M. Bushell, The complexity of miRNA-mediated repression, Cell Death Differ. 22 (1) (2015 Jan) 22–33, https://doi.org/10.1038/cdd.2014.112.

[9] T.G. Ruksha, MicroRNAs' control of cancer cell dormancy, Cell Div. 14 (2019 Oct 10) 11, https://doi.org/10.1186/s13008-019-0054-8.

[10] A. Poniewierska-Baran, S. Słuczanowska-Głąbowska, P. Małkowska, O. Sierawska, Ł. Zadroga, A. Pawlik, P. Niedźwiedzka-Rystwej, Role of miRNA in melanoma development and progression, Int. J. Mol. Sci. 24 (1) (2022 Dec 22) 201, https://doi.org/10.3390/ijms24010201.

[11] A. Poniewierska-Baran, Ł. Zadroga, E. Danilyan, P. Małkowska, P. Niedźwiedzka-Rystwej, A. Pawlik, MicroRNA as a diagnostic tool, therapeutic target and potential biomarker in cutaneous malignant melanoma detection-narrative review, Int. J. Mol. Sci. 24 (6) (2023 Mar 11) 5386, https://doi.org/10.3390/ijms24065386.

[12] N. Lu, J. Min, L. Peng, S. Huang, X. Chai, S. Wang, et al., MiR-297 inhibits tumour progression of liver cancer by targeting PTBP3, Cell Death Dis. 14 (8) (2023 Aug 26) 564, https://doi.org/10.1038/s41419-023-06097-0.

[13] Y. Peng, C.M. Croce, The role of MicroRNAs in human cancer, Signal Transduct. Targeted Ther. 1 (2016 Jan 28) 15004, https://doi.org/10.1038/sigtrans.2015.4.

[14] Y. Yu, Y. Wang, X. Xiao, W. Cheng, L. Hu, W. Yao, et al., MiR-204 inhibits hepatocellular cancer drug resistance and metastasis through targeting NUAK1, Biochem. Cell. Biol. 97 (5) (2019 Oct) 563–570, https://doi.org/10.1139/bcb-2018-0354.

[15] J. Ryan, A. Tivnan, J. Fay, K. Bryan, M. Meehan, L. Creevey, et al., MicroRNA-204 increases sensitivity of neuroblastoma cells to cisplatin and is associated with a favourable clinical outcome, Br. J. Cancer 107 (6) (2012 Sep 4) 967–976, https://doi.org/10.1038/bjc.2012.356.

[16] Z. Bian, L. Jin, J. Zhang, Y. Yin, C. Quan, Y. Hu, et al., LncRNA-UCA1 enhances cell proliferation and 5-fluorouracil resistance in colorectal cancer by inhibiting miR-204-5p, Sci. Rep. 6 (2016 Apr 5) 23892, https://doi.org/10.1038/srep23892.

[17] Q. Wu, Y. Zhao, P. Wang, miR-204 inhibits angiogenesis and promotes sensitivity to cetuximab in head and neck squamous cell carcinoma cells by blocking JAK2-STAT3 signaling, Biomed. Pharmacother. 99 (2018 Mar) 278–285, https://doi.org/10.1016/j.biopha.2018.01.055.

[18] S.G. Wu, T.H. Chang, M.F. Tsai, Y.N. Liu, Y.L. Huang, C.L. Hsu, et al., miR-204 suppresses cancer stemness and enhances osimertinib sensitivity in non-small cell lung cancer by targeting CD44, Mol. Ther. Nucleic Acids 35 (1) (2023 Dec 5) 102091, https://doi.org/10.1016/j.omtn.2023.102091.

[19] X. Wang, S. Rong, Y. Sun, B. Yin, X. Yang, X. Lu, et al., NDRG3 regulates imatinib resistance by promoting β-catenin accumulation in the nucleus in chronic myelogenous leukemia, Oncol. Rep. 50 (2) (2023 Aug) 152, https://doi.org/10.3892/or.2023.8589.
[20] A. Komina, N. Palkina, M. Aksenenko, S. Tsyrenzhapova, T. Ruksha, Antiproliferative and pro-apoptotic effects of MiR-4286 inhibition in melanoma cells, PLoS One 11 (12) (2016 Dec 22) e0168229, https://doi.org/10.1371/journal.pone.0168229.
[21] R. Torres, U.E. Lang, M. Hejna, S.J. Shelton, N.M. Joseph, A.H. Shain, et al., MicroRNA ratios distinguish melanomas from nevi, J. Invest. Dermatol. 140 (1) (2020 Jan) 164–173, https://doi.org/10.1016/j.jid.2019.06.126.
[22] M. Galasso, C. Morrison, L. Minotti, F. Corrà, C. Zerbinati, C. Agnoletto, et al., Loss of miR-204 expression is a key event in melanoma, Mol. Cancer 17 (1) (2018 Mar 9) 71, https://doi.org/10.1186/s12943-018-0819-8.
[23] L. Fattore, G. Cafaro, M. Di Martile, V. Campani, A. Sacconi, D. Liguoro, et al., Oncosuppressive miRNAs loaded in lipid nanoparticles potentiate targeted therapies in BRAF-mutant melanoma by inhibiting core escape pathways of resistance, Oncogene 42 (4) (2023 Jan) 293–307, https://doi.org/10.1038/s41388-022-02547-9.
[24] H. Li, B.B. Yang, Friend or foe: the role of microRNA in chemotherapy resistance, Acta Pharmacol. Sin. 34 (7) (2013 Jul) 870–879, https://doi.org/10.1038/aps.2013.35.
[25] S.Y. Lim, E. Shklovskaya, J.H. Lee, B. Pedersen, A. Stewart, Z. Ming, et al., The molecular and functional landscape of resistance to immune checkpoint blockade in melanoma, Nat. Commun. 14 (1) (2023 Mar 18) 1516, https://doi.org/10.1038/s41467-023-36979-y.
[26] K.J. Livak, T.D. Schmittgen, Analysis of relative gene expression data using real-time quantitative PCR and the 2(-Delta Delta C(T)) Method, Methods 25 (4) (2001 Dec) 402–408, https://doi.org/10.1006/meth.2001.1262.
[27] Y. Chen, Y. Chen, C. Shi, Z. Huang, Y. Zhang, S. Li, et al., SOAPnuke: a MapReduce acceleration-supported software for integrated quality Control and preprocessing of high-throughput sequencing data, GigaScience 7 (1) (2018 Jan 1) 1–6, https://doi.org/10.1093/gigascience/gix120.
[28] A.V. Komina, N.V. Palkina, M.B. Aksenenko, S.N. Lavrentev, A.V. Moshev, A. A. Savchenko, et al., Semaphorin-5A downregulation is associated with enhanced migration and invasion of BRAF-positive melanoma cells under vemurafenib treatment in melanomas with heterogeneous BRAF status, Melanoma Res. 29 (5) (2019 Oct) 544–548, https://doi.org/10.1097/CMR.0000000000000621.
[29] N. Palkina, E. Sergeeva, T. Ruksha, miR 204-5p inhibits apoptosis in DTIC-treated melanoma cells, Oncol. Res. 29 (6) (2022 Nov 10) 393–400, https://doi.org/10.32604/or.2022.025816.
[30] X. Qian, L. Long, Z. Shi, C. Liu, M. Qiu, J. Sheng, et al., Star-branched amphiphilic PLA-b-PDMAEMA copolymers for co-delivery of miR-21 inhibitor and doxorubicin to treat glioma, Biomaterials 35 (7) (2014 Feb) 2322–2335, https://doi.org/10.1016/j.biomaterials.2013.11.039.
[31] N. Amodio, M.T. Di Martino, U. Foresta, E. Leone, M. Lionetti, M. Leotta, et al., miR-29b sensitizes multiple myeloma cells to bortezomib-induced apoptosis through the activation of a feedback loop with the transcription factor Sp1, Cell Death Dis. 3 (11) (2012 Nov 29) e436, https://doi.org/10.1038/cddis.2012.175.
[32] T. Golan, R. Parikh, E. Jacob, H. Vaknine, V. Zemser-Werner, D. Hershkovitz, et al., Adipocytes sensitize melanoma cells to environmental TGF-β cues by repressing the expression of miR-211, Sci. Signal. 12 (591) (2019 Jul 23) eaav6847, https://doi.org/10.1126/scisignal.aav6847.
[33] J. Huang, L. Zhao, Y. Fan, L. Liao, P.X. Ma, G. Xiao, et al., The microRNAs miR-204 and miR-211 maintain joint homeostasis and protect against osteoarthritis progression, Nat. Commun. 10 (1) (2019 Jun 28) 2876, https://doi.org/10.1038/s41467-019-10753-5.
[34] F. Ghini, C. Rubolino, M. Climent, I. Simeone, M.J. Marzi, F. Nicassio, Endogenous transcripts control miRNA levels and activity in mammalian cells by target-directed miRNA degradation, Nat. Commun. 9 (1) (2018 Aug 7) 3119, https://doi.org/10.1038/s41467-018-05182-9.
[35] Y.C. Lin, J.F. Lin, T.F. Tsai, K.Y. Chou, H.E. Chen, T.I. Hwang, Tumor suppressor miRNA-204-5p promotes apoptosis by targeting BCL2 in prostate cancer cells, Asian J. Surg. 40 (5) (2017 Sep) 396–406, https://doi.org/10.1016/j.asjsur.2016.07.001.
[36] C. Li, Q. Ge, J. Liu, Q. Zhang, C. Wang, K. Cui, et al., Effects of miR-1236-3p and miR-370-5p on activation of p21 in various tumors and its inhibition on the growth of lung cancer cells, Tumour Biol 39 (6) (2017 Jun) 1010428317710824, https://doi.org/10.1177/1010428317710824.
[37] L. Zhang, X. Wang, P. Chen, MiR-204 down regulates SIRT1 and reverts SIRT1-induced epithelial-mesenchymal transition, anoikis resistance and invasion in gastric cancer cells, BMC Cancer 13 (2013 Jun 14) 290, https://doi.org/10.1186/1471-2407-13-290.
[38] G. Jiang, L. Wen, H. Zheng, Z. Jian, W. Deng, miR-204-5p targeting SIRT1 regulates hepatocellular carcinoma progression, Cell Biochem. Funct. 34 (7) (2016 Oct) 505–510, https://doi.org/10.1002/cbf.3223.
[39] R. Frazzi, SIRT1 in secretory organ cancer, Front. Endocrinol. 9 (2018 Sep 24) 569, https://doi.org/10.3389/fendo.2018.00569.
[40] F. Yang, Z. Bian, P. Xu, S. Sun, Z. Huang, MicroRNA-204-5p: a pivotal tumor suppressor, Cancer Med. 12 (3) (2023 Feb) 3185–3200, https://doi.org/10.1002/cam4.5077.
[41] Y. Shu, L. Ren, B. Xie, Z. Liang, J. Chen, MiR-204 enhances mitochondrial apoptosis in doxorubicin-treated prostate cancer cells by targeting SIRT1/p53 pathway, Oncotarget 8 (57) (2017 Oct 23) 97313–97322, https://doi.org/10.18632/oncotarget.21960.
[42] A. Lees, T. Sessler, S. McDade, Dying to survive-the p53 paradox, Cancers 13 (13) (2021 Jun 29) 3257, https://doi.org/10.3390/cancers13133257.
[43] H. Yang, B. Yan, D. Liao, S. Huang, Y. Qiu, Acetylation of HDAC1 and degradation of SIRT1 form a positive feedback loop to regulate p53 acetylation during heat-shock stress, Cell Death Dis. 6 (5) (2015 May 7) e1747, https://doi.org/10.1038/cddis.2015.106.
[44] Y. Yu, K. Schleich, B. Yue, S. Ji, P. Lohneis, K. Kemper, et al., Targeting the senescence-overriding cooperative activity of structurally unrelated H3K9 demethylases in melanoma, Cancer Cell 33 (4) (2018) 785, https://doi.org/10.1016/j.ccell.2018.03.009.